Novel role for alphavbeta5-integrin in retinal adhesion and its diurnal peak

Emeline F. Nandrot, Monika Anand, Mousumi Sircar, Silvia C. Finnemann

Am J Physiol Cell Physiol 290: C1256–C1262, 2006.
First published December 7, 2005; doi:10.1152/ajpcell.00480.2005.

Novel role for $\alpha_v\beta_5$-integrin in retinal adhesion and its diurnal peak

Emeline F. Nandrot,[1] Monika Anand,[1] Mousumi Sircar,[1] and Silvia C. Finnemann[1,2,3]

[1]*Margaret M. Dyson Vision Research Institute, Department of Ophthalmology,* [2]*Department of Cell and Developmental Biology, and* [3]*Department of Physiology and Biophysics, Weill Medical College of Cornell University, New York, New York*

Submitted 27 September 2005; accepted in final form 1 December 2005

Nandrot, Emeline F., Monika Anand, Mousumi Sircar, and Silvia C. Finnemann. Novel role for $\alpha_v\beta_5$-integrin in retinal adhesion and its diurnal peak. *Am J Physiol Cell Physiol* 290: C1256–C1262, 2006. First published December 7, 2005; doi:10.1152/ajpcell.00480.2005.—$\alpha_v\beta_5$-Integrin is the sole integrin receptor at the retinal pigment epithelium (RPE)-photoreceptor interface and promotes RPE phagocytic signaling to the tyrosine kinase Mer tyrosine kinase (MerTK) once a day in response to circadian photoreceptor shedding. Herein we identify a novel role for $\alpha_v\beta_5$-integrin in permanent RPE-photoreceptor adhesion that is independent of $\alpha_v\beta_5$'s function in retinal phagocytosis. To compare retinal adhesion of wild-type and *β_5-integrin*$^{-/-}$ mice, we mechanically separated RPE and neural retina and quantified RPE protein and pigment retention with the neural retina. Lack of $\alpha_v\beta_5$-integrin with normal expression of other RPE integrins greatly weakened retinal adhesion in young mice and accelerated its age-dependent decline. Unexpectedly, the strength of wild-type retinal adhesion varied with a diurnal rhythm that peaked 3.5 h after light onset, after the completion of phagocytosis, when integrin signaling to MerTK is minimal. Permanent $\alpha_v\beta_5$ receptor deficiency attenuated the diurnal peak of retinal adhesion in *β_5-integrin*$^{-/-}$ mice. These results identify $\alpha_v\beta_5$-integrin as the first RPE receptor that contributes to retinal adhesion, a vital mechanism for long-term photoreceptor function and viability. Furthermore, they indicate that $\alpha_v\beta_5$ receptors at the same apical plasma membrane domain of RPE cells fulfill two separate functions that are synchronized by different diurnal rhythms.

circadian rhythm; knockout; photoreceptors; retinal pigment epithelium

LIGATION OF INTEGRIN RECEPTORS promotes cellular functions such as substrate adhesion to the extracellular matrix, migration, and phagocytosis. Integrin heterodimers constitute a large family of at least 24 receptors that often share and bind several ligands (20). Studies of integrin function in tissue culture have revealed striking similarities between signaling pathways elicited by integrin receptors during adhesion and during phagocytosis (6). However, matrix adhesion and phagocytosis usually occur at different subcellular domains, at the attached basal surface and at the free apical surface, respectively. Thus adhesive or phagocytic function of a given integrin receptor may be determined by its polarized localization. Alternatively, adhesion and phagocytosis in a given cell type may utilize different integrin family members. For example, macrophages that adhere to laminin via β_1-integrins use apical $\alpha_v\beta_3$-integrin to phagocytose apoptotic cells; adhesion of these cells to the $\alpha_v\beta_3$-integrin substrate fibrinogen redistributes $\alpha_v\beta_3$ basally, diminishing apical phagocytosis (11).

$\alpha_v\beta_5$-Integrin is the only integrin receptor that localizes to the apical surface of the retinal pigment epithelium (RPE) (1, 10). RPE cells form the outermost layer of the retina. Their microvillus-rich apical domain faces the outer segment portions of photoreceptors. Activities of the RPE that are essential for function and survival of photoreceptors include removing aged fragments of photoreceptor outer segments (POS) shed once daily by apical phagocytosis and maintaining contact with intact POS at all times by apical adhesion.

Intraocular pressure and a net fluid transport from retina to RPE likely contribute to retinal adhesion. In addition, apical surface receptors of the RPE are thought to adhere to ligands of the interphotoreceptor matrix (IPM), a complex mix of proteins and proteoglycans that fills the subretinal space and ensheathes outer segment portions of rod and cone photoreceptors (14, 16, 18, 21). IPM proteoglycan rearrangement and RPE microvillus collapse are early responses to retinal detachment that, if persistent, result in RPE dedifferentiation and proliferation, POS degeneration, and photoreceptor cell death (5). Despite their obvious importance for photoreceptor survival and hence vision, we still know little about RPE surface receptors or IPM ligands that may directly mediate retinal adhesion.

The apical surface of the RPE is the sole site of $\alpha_v\beta_5$ expression in the retina. Mice lacking $\alpha_v\beta_5$-integrin develop age-related blindness, illustrating the importance of $\alpha_v\beta_5$ for photoreceptor maintenance (25). Wild-type mice maximize phagocytic activity by 2 h after light onset that triggers rod shedding and barely phagocytose at other times. In contrast, *β_5-integrin*$^{-/-}$ ($\beta_5^{-/-}$) mice lack the daily phagocytic peak but maintain significant phagocytic activity at all times.

In the present study, we set out to test whether lack of apical $\alpha_v\beta_5$-integrin alters retinal adhesion in $\beta_5^{-/-}$ mice compared with strain-matched wild-type ($\beta_5^{+/+}$) mice. We first hypothesized that retinal adhesion may merely be altered at the time of peak $\beta_5^{+/+}$ phagocytosis as a consequence of altered $\beta_5^{-/-}$ phagocytosis. However, we found a robust decrease in retinal adhesion in $\beta_5^{-/-}$ mice at all times of day independent of RPE phagocytic activity. To our knowledge, $\alpha_v\beta_5$-integrin is the first RPE surface receptor directly implicated in retinal adhesion. Retinal adhesion declined with age in both $\beta_5^{-/-}$ and $\beta_5^{+/+}$ mice, suggesting that the age-related vision loss in $\beta_5^{-/-}$ mice is not caused by weak retinal adhesion alone. Finally, our experiments showed that retinal adhesion varied significantly with time of day, peaking daily 3.5 h after light onset in $\beta_5^{+/+}$ mice and to a lesser extent in $\beta_5^{-/-}$ mice. These results reveal a diurnal rhythm of retinal adhesion in mammalian retina that is independent of the rhythm of retinal phagocytosis. Together, these results imply that $\alpha_v\beta_5$-integrin separately mediates both retinal adhesion and phagocytosis at the same plasma membrane domain of the RPE.

MATERIALS AND METHODS

Animals and tissue collection. $\beta_5^{-/-}$ mice characterized in detail previously (19, 25) and $\beta5^{+/+}$ mice of the same genetic background

Address for reprint requests and other correspondence: S. C. Finnemann, Dyson Vision Research Institute, LC305, Box 233, Weill Medical College of Cornell Univ., 1300 York Ave., New York, NY 10021 (e-mail:sfinne@med.cornell.edu).

The costs of publication of this article were defrayed in part by the payment of page charges. The article must therefore be hereby marked "*advertisement*" in accordance with 18 U.S.C. Section 1734 solely to indicate this fact.

(129T2/SvEmsJ; Jackson Laboratory, Bar Harbor, ME) were housed and bred under cyclic 12:12-h light-dark conditions (light onset at 0600) and fed ad libitum. All procedures involving animals were approved by the Weill Medical College Institutional Animal Care and Use Committee.

To quantify retinal adhesion, we modified a protocol described by Endo and colleagues (8). Mice were killed by CO_2 asphyxiation. Lens and cornea were swiftly removed from each enucleated eyeball in HEPES-buffered Hanks' saline solution containing calcium and magnesium. Eyeballs were kept at room temperature to preserve retinal adhesion (8). After transferring an individual eyecup to an empty plastic dish, we performed a single radial cut toward the optic nerve, flattened the eyecup retina facing up, and peeled off the neural retina with forceps from one side of the cut to the other. We stored individual neural retinas and remaining eyecups separately at −80°C. We conducted these tissue harvests in $\beta_5^{+/+}$ and $\beta_5^{-/-}$ mice from 1 to 21 mo of age or at different time points of the light-dark cycle.

Sample lysis. Individual whole eyecups or isolated neural retinas were solubilized in 50 mM Tris·HCl pH 7.5, 2 mM EDTA, 150 mM NaCl, 1% Triton X-100, 0.1% SDS, and 1% NP-40, freshly supplemented with 1% each of protease and phosphatase inhibitor cocktails (Sigma). After separation of insoluble material including melanin pigment by centrifugation, we quantified the protein content of cleared lysates using the Bradford colorimetric assay (4).

RPE pigment quantification. Melanin pigment granules were contained in the insoluble pellet after sample lysis. After washing the pellet in 50% ethanol-50% ether, we dissolved the pellet in 20% DMSO-2 N NaOH at 65°C. We measured absorbance at 490 nm of samples and of commercial melanin pigment (Sigma) at defined concentrations to calculate sample pigment concentrations. We divided pigment concentration by the protein concentration of individual samples to generate a normalized microgram of pigment per milligram of protein concentration in each sample. This accounted for differences among samples in neural tissue yield. Next, we calculated the means ± SE of all samples of each experimental condition. Some samples had outlying normalized pigment concentrations compared with the mean, either because of incomplete harvest and disintegration of the neural retina (abnormally low protein) or because of sample contamination with highly pigmented iris tissue (abnormally high pigment). These samples were excluded from analysis before calculation of final mean pigment values and SEs based on at least three independent retina samples for each condition. We used GraphPad Prism 4.0 software to test for significance with the Student's *t*-test or ANOVA followed by the Bonferroni test as appropriate as indicated in Figs. 1 and 4.

SDS-PAGE and immunoblotting. Immunoblotting analysis was performed only on samples that were included in pigment analysis, as described above. We separated sample lysates representing 15% of one mouse retina or 10% of a whole eyecup in reducing sample buffer on 10% SDS-polyacrylamide gels. After electrophoresis and protein transfer onto nitrocellulose membrane, we immunoblotted with primary antibodies to β_1-integrin (9EG7, provided by D. Vestweber, Max-Planck-Institute of Vascular Biology, Münster, Germany), interphotoreceptor retinoid binding protein [IRBP; provided by B. N. Wiggert, National Institutes of Health (NIH), Bethesda, MD; Ref. 27], neural cell adhesion molecule (N-CAM; provided by E. Rodriguez-Boulan, Weill Medical College), RPE65 (provided by T. M. Redmond, NIH, Bethesda, MD), glial fibrillary acidic protein (GFAP) and ezrin (both from Sigma), α_v- and β_3-integrin (both from BD Pharmingen), β_5-integrin (Santa Cruz Biotechnology, Santa Cruz, CA), and Mer tyrosine kinase (MerTK; R&D Systems) and appropriate horseradish peroxidase-conjugated secondary antibodies followed by chemiluminescence detection (PerkinElmer). X-ray films were scanned, and signals of samples of the same experiment present on the same blot were quantified with NIH Image 1.63 software. We calculated $\beta_5^{-/-}$-to-$\beta_5^{+/+}$ ratios for each experiment, calculated mean ratios and SEs, and tested for significance with Student's *t*-test.

RT-PCR. Total RNA was isolated from individual mouse eyecups with the RNAgent Total RNA isolation system (Promega) and treated with RQ1 DNAse I (Promega) using the manufacturer's protocols. We reverse transcribed 1 μg of mRNA with the Reverse Transcription System (Promega) as instructed. We used cDNA templates to amplify integrin subunits with a custom MultiGene-12 RT-PCR profiling kit (Superarray Biosciences). We used aliquots of the same templates to amplify different regions of the β_5-integrin coding sequence, the neomycin resistance cDNA, and cyclophilin A as an internal control by RT-PCR with the following oligonucleotides: β_5-5′, forward 5′-ACCTCGTGTGAAGAATGCCTG and reverse 5′-CTGGTTAGAGGCTGTGTACTC; β_5-3′, forward 5′-GGAAGTGAGGAAGCAGAGGGTGTCCCGGAACCG and reverse 5′-GACTGTCCCGGAAGCCCACGGGCCTCAAGG; neomycin, forward 5′-CCGGCCGCTTGGGTGGAGAGGC and reverse 5′-GGTCAGCCCATTCGCCGCCAAGC; and cyclophilin, forward 5′-TGGTCAACCCCACCGTGTTCTTCG and reverse 5′-GGTGATCTTCTTGCTGGTCTTGC. After separation of PCR products on 2% agarose 1× Tris-acetate-EDTA gels, we acquired digital pictures of ethidium bromide-treated samples on a GeneFlash apparatus (Syngene Bioimaging).

Immunofluorescence labeling of retinal cryosections. Eight-micrometers-thick frozen sections from paraformaldehyde-fixed eyecups were prepared and stained with antibodies to RPE65 and ezrin and fluorescent secondary antibodies (Molecular Probes) as described previously (10). Images were acquired using a Leica TSP2 confocal microscopy system and recompiled using PhotoShop 7.0 software.

RESULTS

Decreased retinal adhesion in mice lacking $\alpha_v\beta_5$-integrin. Specific receptor-ligand interactions that mediate retinal adhesion are thus far unknown. However, earlier studies found that increased adhesion in amphibian retina precisely coincides with the time of daily peak phagocytosis (7, 24). $\beta5^{-/-}$ mice that are deficient in $\alpha_v\beta_5$-integrin receptors lack the 0800 phagocytosis peak that follows circadian rod outer segment shedding in $\beta_5^{+/+}$ mice ~2 h after light onset at 0600 (25). To test whether reducing phagocytosis alters retinal adhesion, we determined the relative strength of retinal adhesion at 0800 in eyes of age-matched $\beta_5^{+/+}$ and $\beta_5^{-/-}$ mice from 1 to 21 mo of age using established adhesion tests (3, 8). As a consequence of retinal adhesion, whole RPE cells or apical domains of RPE such as microvilli remain attached to the neural retina when the neural retina is peeled off a flattened eyecup. Melanin pigment of the RPE retrieved with isolated neural retina correlates with the extent of RPE attachment to the neural retina, which directly reflects the strength of adhesion between RPE and POS. We observed dense patches of RPE pigment on the outer surface of neural retina peeled off $\beta_5^{+/+}$ mouse eyecups at 0800 (Fig. 1*A*). In contrast, $\beta_5^{-/-}$ retina isolated at 0800 retained dramatically less RPE pigment in all areas, indicating weakened retinal adhesion (Fig. 1*B*). In some $\beta_5^{-/-}$ samples, more RPE pigment was retrieved at the periphery of the retina (data not shown; Ref. 3).

Quantification of solubilized pigment of neural retina samples and normalization to retinal yield showed that significantly less pigment attached to $\beta_5^{-/-}$ retina than to $\beta_5^{+/+}$ retina at 0800, the time of the RPE phagocytosis peak (Fig. 1*C*). This was true for all ages tested, suggesting that lack of $\alpha_v\beta_5$-integrin receptors directly reduces retinal adhesion. Interestingly, pigment retrieved with the neural retina decreased with age in both $\beta_5^{+/+}$ and $\beta_5^{-/-}$ mice. Average pigment content of 12-mo-old neural retina was 45% in $\beta_5^{+/+}$ mice and 34% in

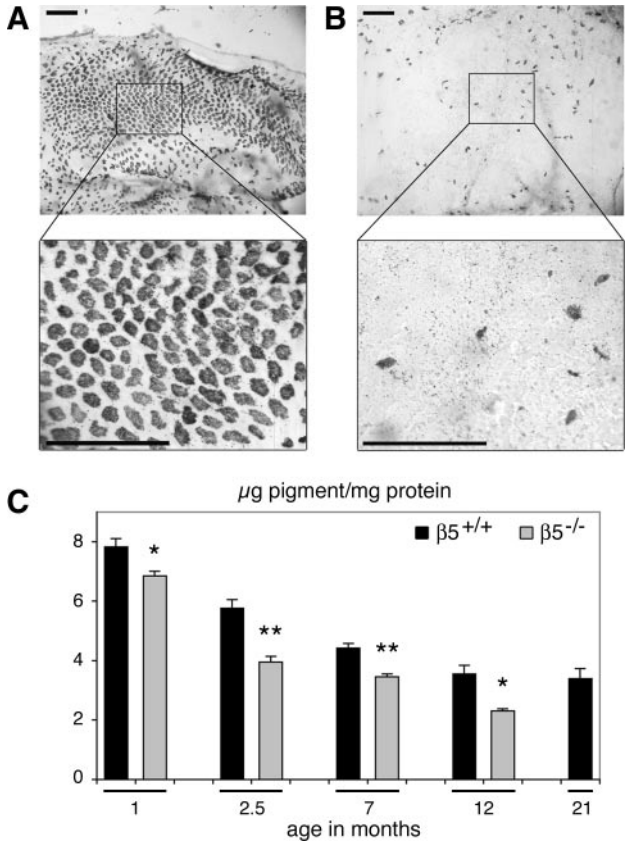

Fig. 1. Decreased retinal pigment epithelium (RPE) pigment adherence to neural retina of β_5-*integrin*$^{-/-}$ ($\beta_5^{-/-}$) mice. *A* and *B*: whole mount bright-field microscopy views of peeled-off retinas with exposed outer retinal surface harvested from 2-mo-old mice. Fields at *bottom* show enlargements of fields at *top*. Scale bars (*top* and *bottom*): 100 μm. *A*: wild-type ($\beta_5^{+/+}$) retina retains dense patches of RPE pigment. *B*: $\beta_5^{-/-}$ retina retains significantly less RPE pigment. *C*: quantification of solubilized RPE pigment peeled off with neural retinas. At all ages tested, $\beta_5^{-/-}$ retina yielded less RPE pigment than $\beta_5^{+/+}$ retina. Furthermore, decreasing amounts of RPE pigment attached to both $\beta_5^{+/+}$ and $\beta_5^{-/-}$ retina with age. Bars represent mean ± SE relative yields of pigment of peeled-off retina; n = 3–5 individual retinas from 2–4 different mice. Significant differences of $\beta_5^{-/-}$ yield compared with $\beta_5^{+/+}$ yield at the same age: *Student's t-test ($P < 0.05$), **Student's t-test ($P < 0.01$).

$\beta_5^{-/-}$ mice compared with 1-mo-old retina of the same genotype (Fig. 1*C*). These data imply that retinal adhesion weakens with age even in $\beta_5^{+/+}$ mice. Lack of $\alpha_v\beta_5$-integrin receptors may accelerate this process: we retrieved 42% less melanin when harvesting neural retina from 2.5-mo-old $\beta_5^{-/-}$ mice than from 1-mo-old $\beta_5^{-/-}$ mice. In contrast, the same difference in age decreased melanin content of neural retina harvested from $\beta_5^{+/+}$ mice by only 26%.

To determine whether increased pigment levels in neural retina samples directly correlate with increased cell transfer and adhesion, we next determined levels of RPE- and retina-specific proteins in extracts of peeled-off neural retinas (Fig. 2*A*). Indeed, we detected higher levels of the RPE-specific protein RPE65 in $\beta_5^{+/+}$ retina extracts than in $\beta_5^{-/-}$ retina extracts harvested from mice from 1 to 12 mo of age (see Fig. 2*A* for representative immunoblots and Table 1 for quantification). The same was true for ezrin, a major constituent of RPE apical microvilli (2). In contrast, we saw no difference in levels of the RPE phagocytosis receptor MerTK, possibly because MerTK expressed in the neural retina may obscure differences in RPE-derived MerTK content. However, $\beta_5^{-/-}$ retina extracts of all ages contained lower levels of α_v-integrin protein than $\beta_5^{+/+}$ extracts and, as expected, no β_5-integrin protein (Fig. 2*A* and Table 1). Similar levels in $\beta_5^{+/+}$ and $\beta_5^{-/-}$ neural retinal extracts of IRBP and GFAP confirmed that both extracts represented the same yield of IPM and neural retina (Table 1). Figure 2*B* shows that the marker proteins we selected, RPE65, ezrin, MerTK, and IRBP, were expressed at equal levels in $\beta_5^{-/-}$ and $\beta_5^{+/+}$ whole eyecups. Low levels of RPE proteins RPE65 and ezrin in neural retina extracts therefore result from poor RPE-retina adhesion in $\alpha_v\beta_5$-integrin-deficient mice.

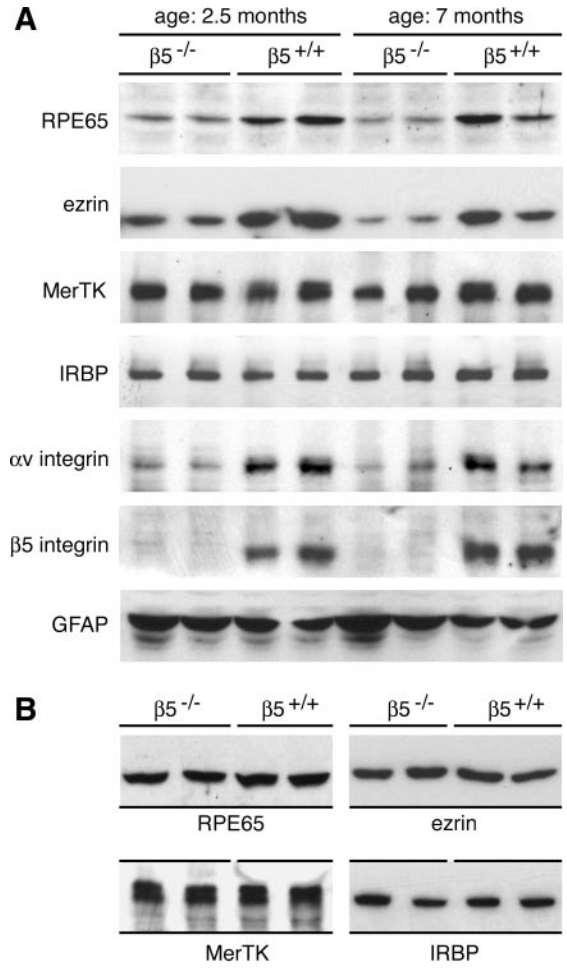

Fig. 2. Decreased content of RPE proteins in peeled-off $\beta_5^{-/-}$ neural retina lysates. *A*: representative immunoblots of peeled-off neural retina lysates harvested from 2.5-mo-old and 7-mo-old mice show reduced amounts of RPE65, ezrin, and α_v-integrin but similar amounts of Mer tyrosine kinase (MerTK), interphotoreceptor retinoid binding protein (IRBP), and glial fibrillary acidic protein (GFAP) in $\beta_5^{-/-}$ lysates compared with $\beta_5^{+/+}$ lysates. As expected, only $\beta_5^{+/+}$ lysates contained β_5-integrin. For quantification of ratios of retrieved $\beta_5^{-/-}$ protein to $\beta_5^{+/+}$ protein, see Table 1. Each lane shows lysate from a different retina. For 2-mo-old mice and 7-mo-old $\beta_5^{-/-}$ mice, samples shown are from both retinas from the same animal. For 7-mo-old $\beta_5^{+/+}$ mice, lanes show retina lysates from 2 different mice. *B*: immunoblots comparing equal fractions of individual whole eyecups of 2-mo-old mice show similar protein expression levels of RPE65, ezrin, MerTK, and IRBP in $\beta_5^{-/-}$ and $\beta_5^{+/+}$ lysates. Lysates from both eyecups of 1 $\beta_5^{+/+}$ and 1 $\beta_5^{-/-}$ mouse are shown. Similar results were obtained by comparing $\beta_5^{-/-}$ with $\beta_5^{+/+}$ lysates from 1-mo-old and 12-mo-old mice (data not shown).

Table 1. *Effect of age on marker protein yield in $\beta_5^{-/-}$ neural retina extracts relative to $\beta_5^{+/+}$ extracts*

Age	RPE65	Ezrin	MerTK	IRBP	α_v-Integrin
1 mo	68±4	64±3	93±4	96±5	58±15
2.5 mo	50±16	53±16	97±12	94±26	51±18
7 mo	65±4	64±15	88±2	98±6	69±8
12 mo	53±8	ND	90±12	104±10	66±13

Values (in %) are means ± SE β_5-*integrin*$^{-/-}$ ($\beta_5^{-/-}$)-to-wild type ($\beta_5^{+/+}$) ratios for each protein. For each protein indicated, 3 separate experiments were performed. For each experiment, 1 retina from 1 mouse of each genotype was lysed and analyzed on the same immunoblot. Band intensities were quantified, and the $\beta_5^{-/-}$-to-$\beta_5^{+/+}$ protein ratio for each protein was calculated. Results from 3 independent experiments were combined to calculate mean ratios. At all ages, retinal pigment epithelium RPE65, ezrin, and α_v-integrin levels in $\beta_5^{-/-}$ extracts were significantly lower than in $\beta_5^{+/+}$ extracts (Student's *t*-test, $P < 0.05$). In contrast, Mer tyrosine kinase (MerTK) and interphotoreceptor retinoid binding protein (IRBP) were present at equal levels in $\beta_5^{-/-}$ and $\beta_5^{+/+}$ samples. ND, not determined.

Reduced levels of α_v-integrin protein but not transcript in $\beta_5^{-/-}$ eyecups. Integrins form a large family of heterodimeric receptors comprised of α- and β-integrin subunits, and at least 24 αβ combinations exist in vertebrates (20). In a given cell, different integrin receptors may share extracellular ligands and have overlapping functions. For instance, we showed previously (11) that macrophages can use either $\alpha_v\beta_3$- or $\alpha_v\beta_5$-integrin to phagocytose apoptotic cells and isolated POS fragments. Therefore, we tested whether expression levels of integrin subunits other than β_5 differed between $\beta_5^{-/-}$ and $\beta_5^{+/+}$ mouse eyecups. First, we compared mRNA levels of four α- and seven β-integrin subunits with a MultiGene-12 RT-PCR profiling kit. Figure 3*A* shows that levels of transcripts of these integrin subunits did not vary greatly between $\beta_5^{-/-}$ and $\beta_5^{+/+}$ eyecups. Notably, this included transcripts of β_5-integrin, because β_5-specific primers of the kit amplified a fragment of the 5′ region of the β_5 cDNA located upstream of the neomycin insertion site of the β_5 targeting construct (Ref. 19 and personal communication with Superarray Biosciences). Because we could not obtain the precise sequence information of the proprietary primer sets included in the MultiGene-12 kit, we performed control RT-PCR amplifications testing β_5 cDNA levels in aliquots of the same templates that we used for the kit reactions. As expected, using primers amplifying a 5′ region that overlaps with the neomycin gene insertion yielded a product only from $\beta_5^{+/+}$ tissue (Fig. 3*B*). In contrast, only $\beta_5^{-/-}$ samples contained the neomycin sequence (Fig. 3*B*). Finally, primers recognizing sequences of the 3′ end of the β_5 cDNA that is untouched by the neomycin insertion amplified products from both $\beta_5^{+/+}$ and $\beta_5^{-/-}$ tissues (Fig. 3*B*). These data confirmed the $\beta_5^{23/-}$ genotype of our β_5-integrin-knockout mice. Furthermore, similar levels of cyclophilin control transcripts in both templates showed that transcripts of β_5-integrin disrupted by the neomycin cassette are present in $\beta_5^{-/-}$ eyecups at steady-state levels similar to those of intact β_5-integrin transcripts in $\beta_5^{+/+}$ eyecups.

Second, we compared expression levels of integrin subunit proteins between $\beta_5^{-/-}$ and $\beta_5^{+/+}$ eyecups (Fig. 3*C*). Using MerTK as a loading control, we found that α_v-integrin protein in $\beta_5^{-/-}$ eyecups decreased by 48 ± 4% compared with $\beta_5^{+/+}$ controls (mean ± SE of 3 individual eyecups from 3 different mice). In contrast, β_1- and β_3-integrins were present at similar steady-state levels in $\beta_5^{-/-}$ and $\beta_5^{+/+}$ eyecups, although both may form integrin receptor dimers with α_v. Finally, $\beta_5^{-/-}$ eyecups contained normal levels of the nonintegrin adhesion receptor N-CAM, whose apical localization in the RPE may depend on RPE-neural retina interaction, as it is lost in RPE in vitro (13). Together, these data indicate that specific reduction of α_v-integrin protein in $\beta_5^{-/-}$ eyecups occurs through post-transcriptional mechanisms. Normal expression levels of other adhesion proteins in $\beta_5^{-/-}$ eyecups suggest that $\alpha_v\beta_5$-integrin receptors may directly mediate retinal adhesion.

Role for $\alpha_v\beta_5$-integrin in a diurnal rhythm of retinal adhesion independent of the rhythm of retinal phagocytosis. The data above show that loss of the synchronized peak of rod POS phagocytosis coincides with decreased retinal adhesion at 0800 in $\beta_5^{-/-}$ retina. At other times of day, phagocytosis continues

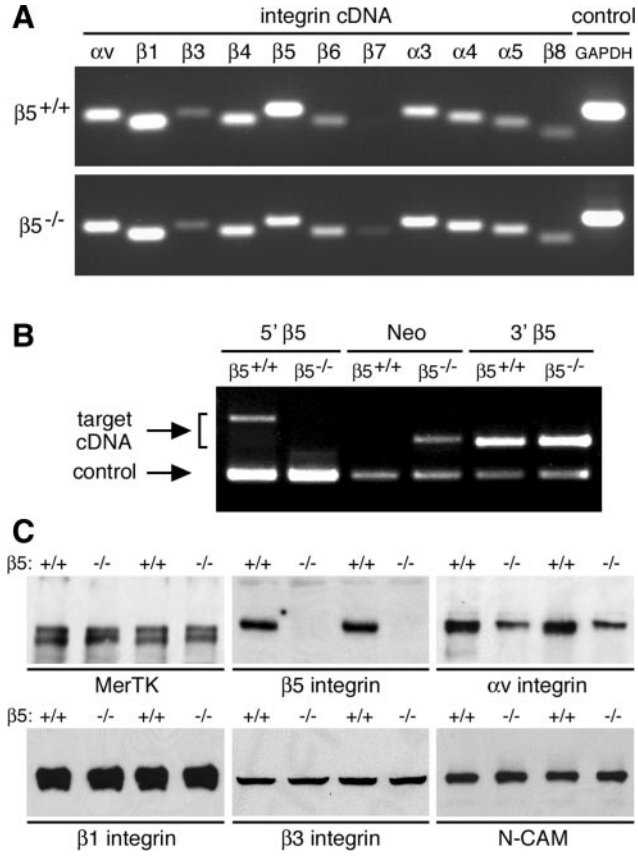

Fig. 3. Comparison of expression of integrin subunits and neural cell adhesion molecule (N-CAM) in $\beta_5^{-/-}$ and $\beta_5^{+/+}$ eyecups. *A*: amplification of integrin-specific cDNA as indicated showed no gross difference in integrin subunit transcript levels when comparing templates prepared from individual 2-mo-old $\beta_5^{-/-}$ and $\beta_5^{+/+}$ eyecups. *B*: amplification of β_5-integrin and neomycin cDNA regions as indicated. Only $\beta_5^{+/+}$ templates possess the 5′ region of the native β_5-integrin cDNA (5′β_5) that is targeted to inactivate the β_5-*integrin* gene in $\beta_5^{-/-}$ mice. Only $\beta_5^{-/-}$ templates include the neomycin selection sequence (Neo). Both templates contain the 3′ region of the β_5-integrin cDNA (3′β_5) that is untouched by neomycin insertion. Cyclophilin was used as an internal control to show equal amounts of cDNA in both templates. *C*: comparative immunoblots of eyecup lysates with primary antibodies as indicated show equal protein levels of β_1-integrin, β_3-integrin, and N-CAM in eyecup lysates prepared from 2-mo-old $\beta_5^{-/-}$ and $\beta_5^{+/+}$ mice. In contrast, $\beta_5^{-/-}$ lysates contained reduced amounts of α_v-integrin and, as expected, no β_5-integrin. Identical levels of MerTK in $\beta_5^{-/-}$ and $\beta_5^{+/+}$ samples confirmed that equivalent fractions of eyecups were loaded. Lysates from individual eyecups of 2 different $\beta_5^{+/+}$ and $\beta_5^{-/-}$ mice are shown.

at equal levels in $\beta_5^{-/-}$ retina, while phagocytosis is essentially absent in $\beta_5^{+/+}$ retina (25). To determine whether phagocytic activity and retinal adhesion directly correlate, we compared $\beta_5^{+/+}$ and $\beta_5^{-/-}$ retinal adhesion at different times of day before and after light onset at 0600. Strikingly, RPE melanin partitioning with the neural retina indicated that retinal adhesion in $\beta_5^{+/+}$ mice varied with time of day, with a distinct peak at 0930 (Fig. 4*A*). Thus retinal adhesion in $\beta_5^{+/+}$ mice was greatest not at the same time as, but subsequent to, the 0800 h peak POS phagocytosis (Fig. 4*A*). Retinal adhesion in mice lacking $\alpha_v\beta_5$-integrin was significantly reduced at all time points tested compared with $\beta_5^{+/+}$ retinal adhesion (Fig. 4*A*). Even in the absence of $\alpha_v\beta_5$, $\beta_5^{-/-}$ retinal adhesion was greater at 0930 than at 0800. However, $\beta_5^{-/-}$ adhesion differed most from $\beta_5^{+/+}$ adhesion at 0930, indicating that $\alpha_v\beta_5$-integrin receptors contribute to the synchronized increase to maximum retinal adhesion in normal retina (Fig. 4*A*). Immunoblots of neural retina extracts probed for RPE and retina markers as shown earlier (Fig. 2) supported the results of the melanin quantification. We previously showed (25) that levels of RPE65 protein in whole retina extracts do not vary with time of earlier day. However, maximum levels of RPE65, ezrin, and β_5-integrin in $\beta_5^{+/+}$ neural retina samples harvested at 0930 h were 1.46 ± 0.14-, 1.44 ± 0.18-, and 1.57 ± 0.06-fold the levels in samples harvested at 0800 (means ± SE of 3–5 individual retinas from 2 or 3 different mice). This clearly demonstrated diurnal variation of retinal adhesion in wild-type mice (Fig. 4*B*). Furthermore, comparative immunoblotting confirmed consistently weaker retinal adhesion and an attenuated phagocytic peak in $\beta_5^{-/-}$ mice (Fig. 4*B*).

Similar peak and nonpeak localization of RPE proteins in $\beta_5^{+/+}$ and $\beta_5^{-/-}$ RPE. It is well known that the composition or spatial organization of molecules in the IPM changes with time of day (28). We therefore tested whether changes in RPE subcellular distribution may contribute to the differential content of RPE65 or ezrin in neural retina extracts that we detected in our adhesion assays. However, the micrographs shown in Fig. 5 demonstrate that neither RPE65 nor ezrin changed its localization in the RPE with time of day (Fig. 5). Furthermore, the distribution of these marker proteins did not differ between $\beta_5^{+/+}$ and $\beta_5^{-/-}$ RPE (Fig. 5). Together, our results therefore identify a diurnal rhythm of retinal adhesion in mammalian retina that depends on $\alpha_v\beta_5$-integrin.

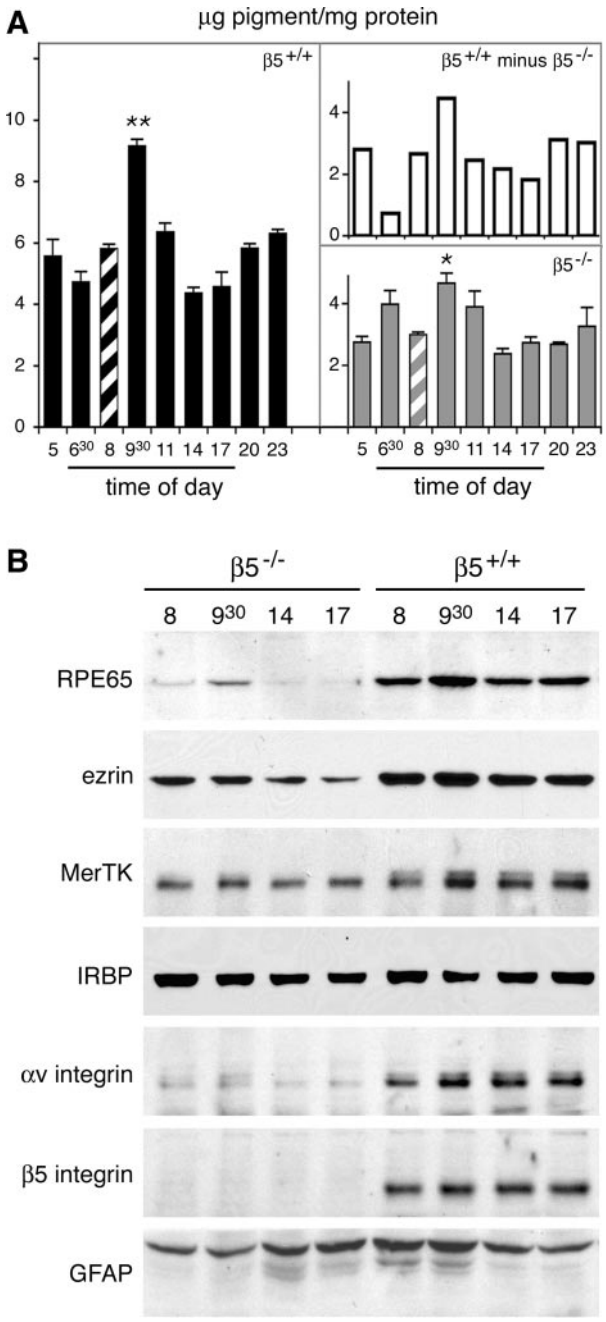

Fig. 4. Attenuation of a diurnal peak in retinal adhesion in $\beta_5^{-/-}$ retina. *A*: RPE pigment content in individual peeled-off neural retina samples from 2-mo-old $\beta_5^{-/-}$ and $\beta_5^{+/+}$ mice killed at different times of day as indicated (light onset at 0600). Filled bars, $\beta_5^{+/+}$ samples; gray bars, $\beta_5^{-/-}$ samples. Open bars show that the reduction in $\beta_5^{-/-}$ pigment content compared with $\beta 5^{+/+}$ pigment content is largest at the time of peak adhesion (0930). Bars represent mean ± SE relative yields of pigment of peeled-off retina; n = 3–5 individual retinas obtained from 2–4 different mice. Significant differences of pigment yield compared with yield at 0800 h (striped bars) of the same genotype: *ANOVA ($P < 0.05$), **ANOVA ($P < 0.001$). Student's t-test indicated significantly less pigment in $\beta_5^{-/-}$ samples compared with $\beta_5^{+/+}$ samples at all time points except 0630 ($P < 0.05$). *B*: representative immunoblots of individual peeled-off neural retina lysates harvested from 2-mo-old mice at times of day as indicated show significantly increased amounts of RPE65 in samples harvested at 0930 compared with other time points. Changes in other marker proteins did not reach significance. Note that RPE65 levels increased significantly in $\beta_5^{-/-}$ samples at 0930 relative to 0800 but remained far below levels of RPE65 in $\beta_5^{+/+}$ samples at any time of day.

DISCUSSION

In this study, we demonstrate a novel role for $\alpha_v\beta_5$-integrin receptors in rhythmic retinal adhesion that is synchronized with the light-dark cycle. To our knowledge, there is no prior report that retinal adhesion varies with time of day in mammalian retina. We considered whether diurnal changes in RPE pigment or protein distribution might contribute significantly to the diurnal differences in their fractionation with neural retina that we interpret as a measure for retinal adhesion. Indeed, melanosomes distribute toward the apical surface of mouse RPE in response to light (12). However, our experiments show that retinal adhesion in wild-type mice increased by 58% from 2 h to 3.5 h after light onset, whereas Futter and colleagues (12) found that the fraction of RPE melanosomes localizing within apical microvilli decreases from 15.5% at 2 h to 5% at 3.5 h after light onset. Furthermore, subcellular distribution of

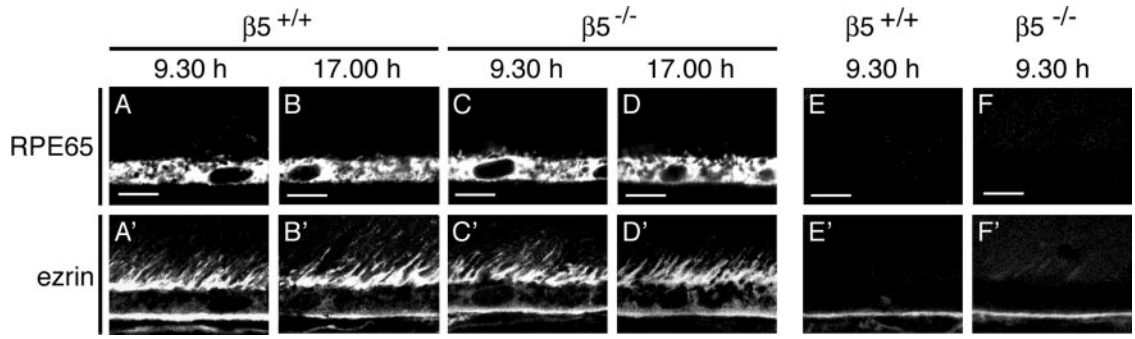

Fig. 5. Similar distribution of RPE65 and ezrin in $\beta_5^{-/-}$ and $\beta_5^{+/+}$ RPE in situ independent of time of day. Double immunofluorescence labeling of retinal cryosections with antibodies to RPE65 (*A–D*) and ezrin (*A′–D′*). Each field shows a representative maximal projection of 1 μm of tissue for comparison of RPE65 and ezrin localization in $\beta_5^{+/+}$ and $\beta_5^{-/-}$ RPE in the eye at 0930 and at 1700 as indicated. Control fields show nonspecific immunofluorescence signals obtained in labeling tissues with secondary antibodies only (*E* and *F* are controls for RPE65; *E′* and *F′* are controls for ezrin). Scale bars are 8 μm.

RPE65 and ezrin did not change from time of peak to nonpeak retinal adhesion in either $\beta_5^{+/+}$ or $\beta_5^{-/-}$ RPE in vivo. Finally, melanin quantification of the neural retina samples correlated very closely with partitioning of the RPE-specific cytoplasmic protein RPE65 with the neural retina. We therefore conclude that differences in retinal adhesion rather than marker mobility are responsible for the differential fractionation of marker pigment and protein we detect.

In frog retina, light onset simultaneously and directly increases both retinal adhesion and POS shedding/RPE phagocytosis (7). In contrast, our time course study reveals that maximal retinal adhesion in mice occurs 1.5 h after maximal POS phagocytosis. Moreover, in preliminary experiments, we found that diurnal changes in retinal adhesion proceed on time even in constant darkness in mice that were previously adapted to normal dark-light fluctuations (data not shown). Like murine POS shedding and phagocytosis, murine retinal adhesion may thus be regulated by circadian rhythms.

Lack of $\alpha_v\beta_5$-integrin abolishes the daily rhythm of POS phagocytosis that restricts RPE phagocytic activity to a period of ~2 h following light onset in normal retina (25). Herein we have demonstrated that lack of $\alpha_v\beta_5$-integrin weakens but does not eliminate RPE-POS adhesion at all times of day and additionally attenuates its synchronized daily fluctuation. Lack of $\alpha_v\beta_5$-integrin receptors may decrease retinal adhesion directly. We found no evidence for expression changes in $\beta_5^{-/-}$ retina of integrin subunits other than β_5's partner subunit α_v or of the cell-cell adhesion receptor N-CAM, whose apical polarity in the RPE requires interaction with photoreceptors (12). Importantly, the difference between $\beta_5^{-/-}$ and $\beta_5^{+/+}$ adhesion was largest precisely at the time of peak adhesion. We conclude that $\alpha_v\beta_5$-integrin contributes to retinal adhesion at all times and is particularly required for strengthening retinal adhesion 3.5 h after light onset.

Phagocytic and adhesive functions of $\alpha_v\beta_5$ receptors at the apical surface of the RPE may be independent of each other, because both are defective immediately after maturation of the retina in $\beta_5^{-/-}$ mice. A precedent for independent regulation of retinal adhesion and POS phagocytosis exists: *vitiligo* mice, which carry a mutation in the microphthalmia transcription factor gene (23), display early-onset retinal detachment that is likely due to a primary defect in retinal adhesion (3). However, *vitiligo* RPE cells in situ phagocytose POS with normal diurnal rhythm, albeit less efficiently than do wild-type RPE cells (22, 26). Thus $\alpha_v\beta_5$-integrin in *vitiligo* RPE may function normally in POS phagocytosis but may not function in, or may not be sufficient for, retinal adhesion.

We previously showed (9, 25) that $\alpha_v\beta_5$-integrin receptors at the apical surface of the RPE initiate a signal transduction pathway via focal adhesion kinase (FAK) that activates the essential phagocytosis receptor MerTK precisely in time for peak phagocytosis 2 h after light onset. It appears unlikely that FAK and MerTK signaling also promote peak adhesion subsequent to phagocytosis, because activities of both kinases in the retina sharply decline before retinal adhesion increases (25). Rather, $\alpha_v\beta_5$ receptors at the same apical surface of the RPE may exist in two independent functional pools that utilize distinct downstream signaling pathways to promote their two distinct functions: POS phagocytosis and retinal adhesion. The highly synchronized $\alpha_v\beta_5$-dependent activities at the RPE-photoreceptor interface provide the ideal in vivo model system to test this intriguing possibility.

Dependence of rhythmic retinal phagocytosis and adhesion on $\alpha_v\beta_5$-integrin suggests that the IPM ensheathing apical RPE microvilli contains ligand proteins for $\alpha_v\beta_5$-integrin that remain to be identified. Both RPE and photoreceptor cells contribute to the IPM that consists of an elaborate and regionalized network of glycoproteins and proteoglycans (16, 17, 21). The $\alpha_v\beta_5$-integrin ligand vitronectin is synthesized by RPE cells in vivo and in vitro but localizes mostly to the basolateral surface of the RPE rather than to the IPM in the retina (15). Interestingly, light-to-dark transition directly stimulates changes in molecular conformation or regional distribution of IPM components in rat retina (28). Studies are under way to identify ligand-$\alpha_v\beta_5$ interactions in retinal adhesion and phagocytosis and to determine whether diurnal changes in ligand availability may contribute to the timely regulation of $\alpha_v\beta_5$ functions in the retina.

ACKNOWLEDGMENTS

We thank Dena Almeida for excellent cryosectioning services and Drs. Thomas M. Redmond, Enrique Rodriguez-Boulan, Dietmar Vestweber, and Barbara N. Wiggert for generously providing antibodies. We also thank Dr. Geri Kreitzer for providing access to the DNA GeneFlash apparatus/gel imaging system.

GRANTS

This work was supported by National Eye Institute Grants EY-13295 and EY-14184. S. C. Finnemann was recipient of a William and Mary Greeve Scholarship by Research to Prevent Blindness, Inc., and of an Irma T. Hirschl Career Scientist Award.

REFERENCES

1. **Anderson DH, Johnson LV, and Hageman GS.** Vitronectin receptor expression and distribution at the photoreceptor-retinal pigment epithelial interface. *J Comp Neurol* 360: 1–16, 1995.
2. **Bonilha VL, Finnemann SC, and Rodriguez-Boulan E.** Ezrin promotes morphogenesis of apical microvilli and basal infoldings in retinal pigment epithelium. *J Cell Biol* 147: 1533–1548, 1999.
3. **Bora N, Defoe D, and Smith SB.** Evidence of decreased adhesion between the neural retina and retinal pigmented epithelium of the *Mitf^{vit}* (*vitiligo*) mutant mouse. *Cell Tissue Res* 295: 65–75, 1999.
4. **Bradford MM.** A rapid and sensitive method for the quantitation of microgram quantities of protein utilizing the principle of protein-dye binding. *Anal Biochem* 72: 248–254, 1976.
5. **Cook B, Lewis GP, Fisher SK, and Adler R.** Apoptotic photoreceptor degeneration in experimental retinal detachment. *Invest Ophthalmol Vis Sci* 36: 990–996, 1995.
6. **Cougoule C, Wiedemann A, Lim J, and Caron E.** Phagocytosis, an alternative model system for the study of cell adhesion. *Semin Cell Dev Biol* 15: 679–689, 2004.
7. **Defoe DM, Matsumoto B, and Besharse JC.** Cytochalasin D inhibits L-glutamate-induced disc shedding without altering L-glutamate-induced increase in adhesiveness. *Exp Eye Res* 48: 641–652, 1989.
8. **Endo EG, Yao XY, and Marmor MF.** Pigment adherence as a measure of retinal adhesion: dependence on temperature. *Invest Ophthalmol Vis Sci* 29: 1390–1396, 1988.
9. **Finnemann SC.** Focal adhesion kinase signaling promotes phagocytosis of integrin-bound photoreceptors. *EMBO J* 22: 4143–4154, 2003.
10. **Finnemann SC, Bonilha VL, Marmorstein AD, and Rodriguez-Boulan E.** Phagocytosis of rod outer segments by retinal pigment epithelial cells requires $\alpha_v\beta_5$ integrin for binding but not for internalization. *Proc Natl Acad Sci USA* 94: 12932–12937, 1997.
11. **Finnemann SC and Rodriguez-Boulan E.** Macrophage and retinal pigment epithelium phagocytosis: apoptotic cells and photoreceptors compete for $\alpha_v\beta_3$ and $\alpha_v\beta_5$ integrins, and protein kinase C regulates $\alpha_v\beta_5$ binding and cytoskeletal linkage. *J Exp Med* 190: 861–874, 1999.
12. **Futter CE, Ramalho JS, Jaissle GB, Seeliger MW, and Seabra MC.** The role of Rab27a in the regulation of melanosome distribution within retinal pigment epithelial cells. *Mol Biol Cell* 15: 2264–2275, 2004.
13. **Gundersen D, Powell SK, and Rodriguez-Boulan E.** Apical polarization of N-CAM in retinal pigment epithelium is dependent on contact with the neural retina. *J Cell Biol* 121: 335–343, 1993.
14. **Hageman GS, Marmor MF, Yao XY, and Johnson LV.** The interphotoreceptor matrix mediates primate retinal adhesion. *Arch Ophthalmol* 113: 655–660, 1995.
15. **Hageman GS, Mullins RF, Russell SR, Johnson LV, and Anderson DH.** Vitronectin is a constituent of ocular drusen and the vitronectin gene is expressed in human retinal pigmented epithelial cells. *FASEB J* 13: 477–484, 1999.
16. **Hollyfield JG.** Hyaluronan and the functional organization of the interphotoreceptor matrix. *Invest Ophthalmol Vis Sci* 40: 2767–2769, 1999.
17. **Hollyfield JG, Varner HH, and Rayborn ME.** Regional variation within the interphotoreceptor matrix from fovea to the retinal periphery. *Eye* 4: 333–339, 1990.
18. **Hollyfield JG, Varner HH, Rayborn ME, and Osterfeld AM.** Retinal attachment to the pigment epithelium. *Retina* 9: 59–68, 1989.
19. **Huang X, Griffiths M, Wu J, Farese RV Jr, and Sheppard D.** Normal development, wound healing, and adenovirus susceptibility in β5-deficient mice. *Mol Cell Biol* 20: 755–759, 2000.
20. **Hynes R.** Integrins: bidirectional, allosteric signaling machines. *Cell* 110: 673–687, 2002.
21. **Johnson LV and Hageman GS.** Structural and compositional analyses of isolated cone matrix sheaths. *Invest Ophthalmol Vis Sci* 32: 1951–1957, 1991.
22. **Kosaras B and Sidman RL.** Phagosome number and distribution in retinal pigment epithelial cells of vitiligo mutant mice. *Exp Eye Res* 63: 151–158, 1996.
23. **Lamoreux ML, Boissy RE, Womack JE, and Nordlund JJ.** The *vit* gene maps to the mi (microphthalmia) locus of the laboratory mouse. *J Hered* 83: 435–439, 1992.
24. **Matsumoto B, Defoe DM, and Besharse JC.** Membrane turnover in rod photoreceptors: ensheathment and phagocytosis of outer segment distal tips by pseudopodia of the retinal pigment epithelium. *Proc R Soc Lond B Biol Sci* 230: 339–354, 1987.
25. **Nandrot EF, Kim Y, Brodie SE, Huang X, Sheppard D, and Finnemann SC.** Loss of synchronized retinal phagocytosis and age-related blindness in mice lacking $\alpha_v\beta_5$ integrin. *J Exp Med* 200: 1539–1545, 2004.
26. **Smith SB, Cope BK, McCoy JR, McCool DJ, and Defoe DM.** Reduction of phagosomes in the vitiligo (C57BL/6-mi^{vit}/mi^{vit}) mouse model of retinal degeneration. *Invest Ophthalmol Vis Sci* 35: 3625–3632, 1994.
27. **Smith SB, McClung J, Wiggert BN, and Nir I.** Delayed rhodopsin regeneration and altered distribution of interphotoreceptor retinoid binding protein (IRBP) in the mi^{vit}/mi^{vit} (vitiligo) mouse. *J Neurocytol* 26: 605–613, 1997.
28. **Uehara F, Matthes MT, Yasumura D, and LaVail MM.** Light-evoked changes in the interphotoreceptor matrix. *Science* 248: 1633–1636, 1990.